International Journal of Research in Engineering and Science (IJRES)
ISSN (Online): 2320-9364, ISSN (Print): 2320-9356
www.ijres.org Volume 13 Issue 4 ǁ April 2025 ǁ PP. 178-188

Construction of a visual exosome-mediated delivery system across the blood-brain barrier

Qi Tan[1], Tingting Yu[1,2], Meili Hou[1,2], Yi Liu[1,2*], Nan Hu[1,2*]
[1] *College of Chemical Engineering, Sichuan University of Science & Engineering, Zigong 643002, China*
[2] *Institute of Precision Medicine, Zigong Academy of Big Data and Artificial Intelligence in Medical Science, Zigong Fourth People's Hospital, Zigong 643000, China*
**Corresponding Author: Nan Hu, E-mail: susehn@163.com; Yi Liu, E-mail: yiliu@suse.edu.cn*

ABSTRACT*: Central nervous system (CNS) disorders have a high prevalence worldwide, which have no effective treatment, largely due to the blood-brain barrier (BBB) hindering drug delivery. Exosome-based drug delivery systems have unique therapeutic advantages due to their low immunogenicity and BBB penetration potential. In this study, we developed a visualized exosome-based drug delivery system and validated its reliability. We constructed GFP-coupled rabies virus glycoprotein (RVG) peptide-modified RVG-GFP-exos and established a stable transactivation cell line that stably secreted the exosomes. By loading GAPDH siRNA and doxorubicin hydrochloride, respectively, we tested the targeting ability of RVG-GFP-exos and GFP-exos in bEnd.3 cells and their penetration in a BBB model in vitro. The results showed that the cellular uptake efficiency of the RVG-GFP-exo group increased 3.25-fold compared with the unmodified group ($p < 0.001$), and its GAPDH siRNA knockdown efficiency reached 53%, which was significantly higher than control group ($p < 0.01$). In addition, the RVG-GFP-exo group exhibited significantly higher transmigration across the in vitro BBB model ($p < 0.001$). In conclusion, we successfully constructed a brain-targeted drug delivery system based on engineered exosomes, showed its targeting ability and providing a reliable preclinical and experimental basis for the precise treatment of neurodegenerative diseases.*

KEYWORDS*: Exosomes, RVG, BBB, drug delivery, neurodegenerative disease*

Date of Submission: 08-04-2025 Date of acceptance: 19-04-2025

I. INTRODUCTION

Diseases of the central nervous system (CNS), such as Alzheimer's disease (AD), Parkinson's disease (PD), and glioblastoma, are increasingly prevalent in the elderly population and represent the category of diseases with the highest disability rates worldwide [1]. The number of patients with AD is expected to exceed 139 million in 2050. The key bottleneck constraining the treatment of CNS diseases is the physiological barrier property of the blood-brain barrier (BBB), a selectively permeable interface formed by the endothelial cells of cerebral microvessels through tight junctions, which results in more than 98% of small-molecule drugs and almost all large-molecule therapeutic agents, including recombinant proteins, monoclonal antibodies, and gene drugs, being unable to cross the BBB [2,3]. Therefore, developing novel drug delivery systems with efficient BBB penetration and precise targeting has become a core scientific issue to overcome the therapeutic dilemma of neurodegenerative diseases.

Exosomes, as natural extracellular vesicles with a diameter of 30–150 nm, can carry nucleic acids and proteins from donor cells to be transported to proximal or distal recipient cells to alter their function or physiological state [4]. Exosomes have several unique biological properties: endogenous characteristics confer excellent biocompatibility and immune escape ability; the amphiphilic phospholipid bilayer structure can load hydrophilic (siRNA) and hydrophobic drugs (Adriamycin) simultaneously; and surface protein modifications can mediate trans-BBB translocation, allowing neuron-derived exosomes to achieve targeted delivery through the specific binding of the integrin LFA-1 to the cerebral vascular endothelial ICAM-1 [5]. Compared with adeno-associated virus (AAV) vectors, exosomes not only have higher drug-carrying capacity (> 100 nm particle size) but can also deliver functional mRNAs directly through the membrane fusion mechanism. Exosomes have high stability, are easy to store, and can be used for long-distance drug delivery under physiological or pathological conditions [6]. As an ideal class of drug delivery carriers, exosomes provide a rich range of innovative solutions for CNS drug delivery.

Currently, there are two main modes of exosome-based CNS drug delivery. One such mode involves utilizing natural exosomes produced by the body's cells with BBB penetrating ability, such as those secreted by M2 macrophages that can be taken up by neuronal cells in vitro and in vivo [7]. The extent to which natural exosomes penetrate the BBB depends on their surface ligands being recognized by brain vascular endothelial cell-

associated receptors. However, this kind of natural exosomes lack targeting; only a small part of the exosomes can penetrate the BBB and reach the brain. Most of the exosomes are enriched in the human liver or other organs and are quickly cleared out of the body through bile excretion, kidney filtration, and phagocytosis of the reticuloendothelial system. The other mode involves the preparation of engineered exosomes capable of penetrating the BBB through specific modification. A team of researchers from the University of Oxford, UK, expressed the exosome membrane protein Lamp2b in fusion with the neuron-specific rabies virus glycoprotein (RVG) to enable cells to secrete engineered exosomes with the RVG tag, which allowed the exosomes to target brain tissues by binding to the nicotinic acetylcholine receptor [8].

Exosomes as drug delivery carriers have become a significant research area. Although exosomes possess the advantages of large loading capacity, non-immunogenicity, and high targeting, exosome drug delivery technology still faces many problems, such as the difficulty of purifying natural exosomes, the difficulty of targeting exosome modification, and the difficulty of optimizing the production process of medicinal exosomes.

The highly neurophilic RVG can deliver nucleic acids, proteins, and other molecules to specific cells, such as brain microvascular endothelial cells, the thalamus, striatum, hippocampus, and cortex, by specifically binding to nicotinic acetylcholine receptors in various structures of the CNS and crossing the BBB through the transcytosis pathway, which reduces the non-specific uptake of drugs and drug toxicity [9–12]. Consequently, various CNS delivery strategies based on RVG modification have been reported. For instance, RVG can be specifically modified to form chimeric peptides, which increase its binding ability to siRNAs and allow the chimeric peptides carrying disease-associated specific siRNAs to be targeted to neuronal cells for drug delivery. RVG can be fused with other peptides through protein fusion technology, which can provide protein therapies for CNS diseases. In addition, RVG can be used for specific modification of engineered exosomes or engineered nanoparticles to increase their brain tissue targeting ability. Therefore, RVG modification has a promising future for drug-targeted delivery for CNS diseases [13–16].

In this study, based on the tetracycline-inducible lentiviral expression system (Lenti-X Tet-On), we have innovatively constructed RVG-modified engineered exosomes (RVG-exo) with dual labeling (green fluorescent protein (GFP)/HA tag protein) and aimed to elucidate the following through comparative experiments: (i) the modulation of the efficacy of RVG modification in exosome targeting; (ii) the difference in delivery efficiency of exosomal drugs (siRNA); and (iii) the transport kinetic characteristics of engineered exosomes in an in vitro BBB model. In this study, we established a complete technical system, from vector construction and target modification to functional validation, which provides a new methodological framework and preclinical foundation for precision therapy for neurodegenerative diseases.

II. MATERIALS AND METHODS

2.1. Reagents and chemicals. All plasmids involved in the article were purchased from Wuhan Miaoling Biotechnology Co., Ltd (Wuhan, China). KOD-Plus-Neo high-fidelity polymerase was purchased from TOYOBO (Japan). EcoR Ⅰ, BamH Ⅰ fast cleavage enzyme, and BeyoRT™ III cDNA synthesis pre-mix were purchased from Shanghai Beyotime Biotechnology Co. Fetal bovine serum (FBS) was purchased from Sangong Bioengineering Co Ltd (Shanghai, China). Puromycin, doxycycline, Polybrene, Adriamycin hydrochloride, Adazol total RNA extraction reagent, and DMEM high glucose medium (ATCC modified) were purchased from Shanghai Titan Technology Co Ltd (Shanghai, China). Human embryonic kidney cells (HEK-293), mouse brain microvascular endothelial cells (bEnd.3), and DMEM low bicarbonate basal medium were purchased from iCell Bioscience (Shanghai, China). CD63, HA, GFP primary antibody, and Alexa Fluor 647 fluorescent secondary antibody were purchased from Sangong Bioengineering Co. GAPDH and β-tubulin primary antibodies were purchased from Kantor Antibody Technology (Wuhan) Co Ltd (Wuhan, China). Calnexin primary antibody, TSG101 primary antibody, Lipo293™ transfection reagent, Lipo6000™ transfection reagent, 4% paraformaldehyde fixative, FITC-labelled Dextran (MW40,000), antiFluorescence Quenching Blocking Solution, BCA Protein Concentration Assay Kit, and Ultrasensitive ECL Chemiluminescence Kit were purchased from Shanghai Beyotime Biotechnology Company Limited (Shanghai, China). The mouse GAPDH, ACTB internal primers and GAPDH siRNA (Sense (5'-3'): CACUCAAGAUUGUCAGCAATT; Antisense (5'-3'): UUGCUGACAAUCUUUGAGUGAG) that we ordered were purchased from Sangong Bioengineering Co. Cytotoxicity detection kit (CCK-8) was purchased from APExBIO (USA). 2✕SP qPCR mix was purchased from Chongqing Baoguang Biotechnology Co.

2.2. Plasmid construction and transfection. We generated two recombinant plasmid variants (RVG-containing and RVG-deficient) through PCR-mediated tandem linkage of RVG, EGFP, and HA sequences to the exosomal membrane protein Lamp2b, followed by homologous recombination. RVG and EGFP were fused to the N-terminal domain of Lamp2b, enabling their surface display on exosomal membranes. HEK-293 cells were seeded in six-well plates at a density of 2×10^5 cells/well and cultured for 24 hours to achieve 60-70% confluence prior to transfection. Plasmid transfection was then performed using the liposomal transfection reagent Lipo293™ (Beyotime Biotechnology, China).

2.3. Cell culture. HEK-293 cells were maintained in high-glucose DMEM supplemented with 10% FBS and 1% penicillin/streptomycin. Exosome-depleted FBS was prepared via ultracentrifugation at 120,000 × g for 14 h at 4°C, followed by supernatant collection through 0.22-μm filtration. HEK-293 cells at 80% confluence were cultured in exosome-depleted medium (DMEM containing 10% processed FBS) for 72 h. Conditioned medium was subsequently collected and centrifuged at 300 × g for 10 min to remove cellular debris. bEnd.3 murine endothelial cells were cultured in low-glucose DMEM (1.0 g/L D-glucose) supplemented with 10% FBS, under standard culture conditions (37°C, 5% CO_2, 95% humidity).

2.4. Preparation and characterization of exosomes from HEK-293 cells. HEK-293 exosomes were collected from the culture medium by differential centrifugation. Briefly, the medium is centrifuged at 300×g for 10 minutes at 4 °C after culturing the cells for 72 hours. Then, the supernatant is centrifuged at 3000×g for 10 minutes at 4 °C to complete the initial enrichment. The supernatant was centrifuged at 10,000×g ultracentrifugation at 4 °C for 1 h. Cells and debris were removed using a 0.22-μm filter (Millipore). The supernatant was ultracentrifuged at 120,000×g for 2 h, and the precipitate was resuspended in phosphate-buffered saline (PBS) and ultracentrifuged again at 120,000×g for 2 h. Finally, the exocytosis of the cells obtained from the HEK-293 precipitate was resuspended in 200 μL of phosphate-buffered saline (PBS) and used for the subsequent experiments. Analyses were performed by using transmission electron microscopy and nanoparticle tracking. Exonic surface markers (CD63 and TSG101) were identified using Western blotting.

2.5. Steady-turn cell line construction. To enable rapid exosome production and cost-effective high-yield expression, we employed a lentiviral Lenti-X Tet-One-Puro inducible expression system to establish stably transduced cell lines. Primary constructs were generated through molecular cloning of RVG-EGFP-Lamp2b-HA and EGFP-Lamp2b-HA sequences into pLVX-TetOne vectors, yielding pLVX-TetOne-Puro-RVG-EGFP-Lamp2b-HA and pLVX-TetOne-Puro-EGFP-Lamp2b-HA plasmids. HEK-293 cells were seeded in six-well plates at a density of 2×10^5 cells/well 24 hours prior to transfection, achieving 60-70% confluence at the time of transfection. The lentiviral transfer plasmids were co-transfected with packaging plasmids pMD2.G and psPAX2 at a 4:1:3 molar ratio using Lipo293TM liposomal transfection reagent. Following transfection, the cells were cultured for an additional 72 hours, after which the supernatant was collected. The supernatant was clarified by centrifugation at 300×g for 5 minutes, followed by 20-fold concentration using 100 kDa molecular weight cut-off ultrafiltration membranes, yielding lentiviral particle-enriched concentrates.For lentiviral transduction, HEK-293 cells were plated in complete growth medium to attain 70-80% confluence in six-well plates. Transduction was enhanced with 6 μg/mL polybrene. Following 24-hour transduction, the viral medium was aspirated and replaced with complete growth medium. Cells were maintained for 48 hours post-transduction to enable transgene integration. Puromycin selection (4 μg/mL) was initiated at subconfluent densities (<25% confluence). Medium was refreshed every 48 hours during the 7-14 day selection period. Stable polyclonal populations were subsequently expanded for doxycycline-induced expression and subsequent exosome characterization.

2.6. loading of cargoes in exosomes. To obtain exosome particles loaded with GAPDH siRNA and adriamycin hydrochloride respectively, we used the electroporation method, where the purified exosome particles were mixed with the two kinds of cargoes at a ratio of 1:1 (Wt/Wt) respectively (the concentration of exosomes was not more than 0.5 μg/μL), added into a 0.4cm electroshocking cup, and electroporated into the mixture with a capacitance of 400V and 125uF (pulse duration 10-15ms) the mixture was electroporated at 400ul each time. After electroporation, it was left at 37°C for 20 minutes to allow recovery of the exosome membrane structure, and then, the precipitate was repurified using Exo-Quick.

2.7. CCK-8 Assay. We used a CCK-8 assay to evaluate the cytotoxicity of exosomes. Initially, bEnd.3 cells were inoculated in 96-well plates overnight to promote cell attachment. Exosome complexes (PBS, exosome loaded with GAPDH siRNA (Exo/siRNA), exosome modified with RVG and loaded with GAPDH siRNA (RVG-exo/siRNA)) at different concentrations (0, 12.5, 25, 50, 100 μg/mL) were added to transwell inserts and co-cultivated with cells for 24 hours. After co-culture, CCK-8 reagent was added to each well, and absorbance was measured at 450 nm using an microplate reader.

2.8. In vitro cellular uptake experiments. According to our experimental design, high expression of green fluorescent protein (GFP) and HA-tagged proteins on both exosomes obtained was indeed confirmed by protein immunoblotting. One hundred thousand mouse micro cerebral vascular endothelial cells (bEnd.3) were inoculated in 24-well plates containing cell crawls for overnight incubation, followed by co-incubation of the two exosomes, RVG-exos and Exosomes, respectively, with the cells at a final concentration of 100 μg/mL for 24 h. The medium was discarded and the cells were fixed with 4% paraformaldehyde and permeabilized with 0.1% Tritonx-100 using 5% BSA for sealing, followed by incubation of cell crawls with rabbit anti-HA primary antibody (1:200 dilution) overnight (4°C), followed by washing at each step, followed by incubation of cell crawls with goat anti-rabbit Alexa Fluor 647 fluorescent secondary antibody at room temperature for 1h, washing, and finally staining of the nuclei using Hoechst 33258, sealing, and then observing the cell fluorescence by inverted fluorescence microscope.

2.9. Quantitative reverse transcription PCR. The bEnd.3 cells were inoculated at a density of 1×10^5 cells/well in 6-well plates containing culture medium. These cells were treated with RVG-exos/siRNA or Exos/siRNA for

48 h. Total RNA was extracted using TRIzol reagent to detect the expression of GAPDH sequences, and we synthesized miRNA first-strand cDNA using the miRNA Tail Reaction First Strand cDNA Synthesis Kit according to the manufacturer's instructions. ACTB was used as an internal reference control. Expression levels were determined using the $2^{-\Delta\Delta CT}$ method.

2.10. Western blotting. Total cellular proteins were extracted and subjected to immunoblotting after treating the cells with RVG-exos/siRNA and Exos/siRNA for 48 h. Western blotting was performed to detect the level of the GAPDH. After extraction of total proteins, an aliquot (20 μg) of the extracted protein samples was sampled and separated on a sodium dodecyl sulfate-polyacrylamide gel and transferred to a 0.4-μm NC membrane (Millipore). The membranes were closed with 5% skimmed milk for 1 h at RT (25°C), then incubated with primary antibodies against GAPDH (1:10,000) and α-tubulin (1:10,000) overnight at 4°C, followed by incubation with secondary antibodies for 1 h at RT. Finally, protein bands were visualized using an ultrasensitive ECL chemiluminescence kit to analyze protein expression levels.

2.11. In vitro BBB modeling. To establish the in vitro BBB model, transwell chambers (24-well plates) consisting of 0.4-μm polyester membranes were used. We inoculated the upper chamber with 1×10^5 bEnd.3 cells and filled the lower chamber with 600 μL of complete medium, changed the fluid daily in the small chamber and every two days in the outer chamber, and continued the culture for 7 days before starting to validate the integrity of the BBB model. We made the height difference between the liquid level of the small chamber and the outer chamber page greater than 0.5cm and observed whether the liquid level difference changed after 12h overnight. We then used FITC-labelled Dextran (MW40,000) to assess the permeability of the BBB model. We added a final concentration of 0.5 mg/mL of FITC-labelled Dextran to the upper chamber and 600 μL of complete medium to the lower chamber and placed them in the incubator for 1 h. After one h of incubation, samples were extracted from the upper and lower chambers respectively, and FITC fluorescence intensity assays were performed (Absorption Peak: 492 nm; Emission Peak: 520 nm), and a standard curve was made to calculate the FITC-labelled Dextran concentration. The BBB membrane permeability was calculated according to the formula $Papp=(dQ/dt)\ (\ 1/C_0\ )\ (1/A)$, where dQ/dt is the permeability, C_0 is the initial concentration in the donor compartment, and A is the surface area of the filter [17].

2.12. Transwell experiment. In order to verify whether our constructed engineered exosomes can cross the blood-brain barrier and whether the RVG modification can enhance their ability to cross the blood-brain barrier, we performed Transwell experiments. Two types of exosomes, RVG-exos/DOX and Exos/DOX, were prepared by encapsulating adriamycin hydrochloride (DOX) into exosomes by electrotransformation. RVG-exos/DOX and Exos/DOX were added into the chambers of the constructed-in vitro BBB model at a concentration of 100 μg/mL, and the intensity of adriamycin fluorescence in the lower chamber was detected (excitation wavelength of 470 nm and emission wavelength of 590 nm) at 0, 6, 12, and 24 hours, respectively.

2.13. Statistical Analysis. Data are presented as the mean ±standard deviation (SD) of at least three independent experiments. A student's t-test was used for pairwise comparisons and ANOVA with Dunnett's post hoc test was used to compare three or more groups. Statistical significance was defined at $P \leq 0.05$. All statistical analyses were performed using GraphPad Prism 7.0.

III. RESULTS

3.1. Preparation and characterization of exosomes from HEK-293 cells. Two recombinant plasmids were constructed by genetic engineering (Figure 1A) and then transfected into HEK-293 cells to obtain engineered exosomes. Because the plasmids carried genes expressing GFP proteins, green fluorescence was observed under a fluorescence microscope 72 h after transfection (Figure 1C). The structure of the intra- and extra-membrane distributions of the modified proteins on exosomes was determined from protein conformation prediction (Figure 1B). The exosome-specific protein TSG101 was detected in both RVG-modified exosomes and unmodified exosomes (Figure 1F), and the results of NTA showed that the average diameter of RVG-modified exosome particles was 149.6 nm, while that of unmodified exosome particles was 157.1 nm (Figure 1E). In addition, transmission electron microscope (TEM) revealed that these two exosomes exhibited typical cup- and bowl-shaped structures (Figure 1D). Immunoblotting for modified proteins on the obtained exosomes revealed GFP and HA expression on both exosomes, as expected (Figure 1G).

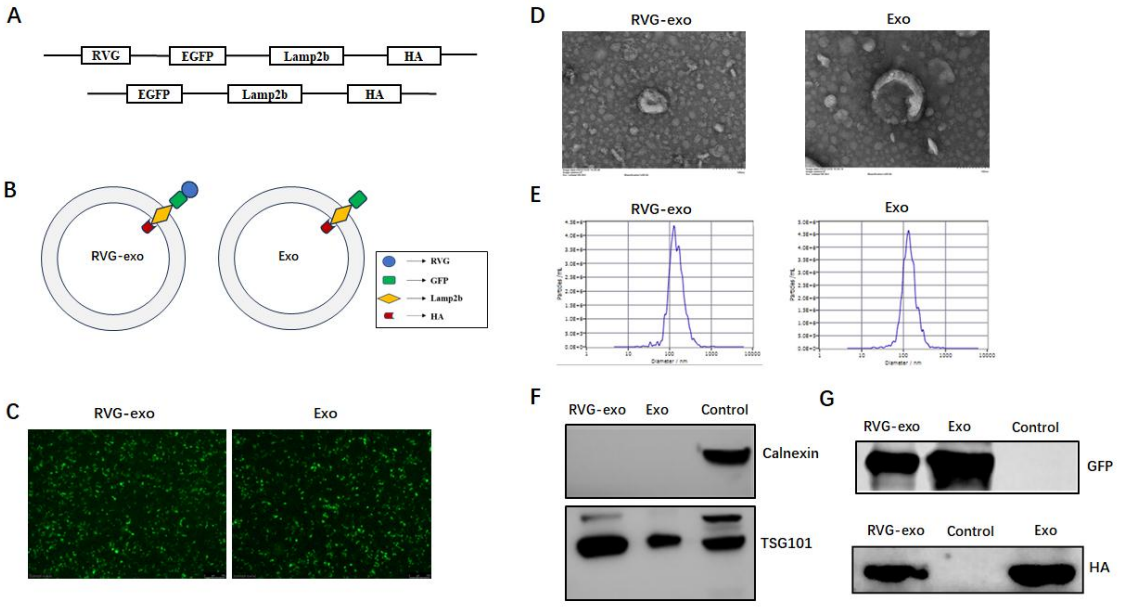

Figure 1. Recombinant plasmid construction and characterization of transfected and human embryonic kidney cell-derived exosomes. (A) Construction of two recombinant plasmids to generate engineered exosomes. (B) Distribution of modified proteins on engineered exosomes generated by recombinant plasmids. (C) Fluorescence expression of cells under a fluorescence microscope 72 h after transfection with the recombinant plasmid. (D) Transmission electron microscope (TEM) observation of exosome morphology. Scale bar: 100 nm. (E) Nanoparticle tracking analysis (NTA) measurement of exosome size. (F) Western blot analysis of marker proteins in exosomes. Control: HEPG2 cells; RVG-exo/Exo: exosomes. (G) Western blot of modified peptides on engineered exosomes. Control: HEK-293 cells; RVG-exo/Exo: exosomes.

3.2. Identification and characterization of HEK-293 stably transduced cells and their exosomes. To obtain a large number of exosomes in a short period of time and at a low cost while ensuring the high production of exosomes, we used a lentivirus-based Lenti-X Tet-One-Puro inducible expression system to construct a stable cell line. Puromycin screening was performed after lentiviral transduction; this resulted in massive cell death during the pre-screening period, which stabilized after 3 days with normal cell growth. HEK-293 cells were spread on the plate after puromycin screening, and pronounced green fluorescence was observed in the cells under doxycycline induction, and apparent green fluorescence was observed in the cells under doxycycline induction. No green fluorescence was expressed under non-induction (Figure 2A). The green fluorescent protein (GFP) was stably expressed within 72 h, and obvious green fluorescence was observed after passaging and continued induction. Western blot analysis of two cell lines showed that the target protein was expressed under doxycycline induction, while no target protein was expressed without doxycycline induction (Figure 2B). We characterized the exosomes produced by this stable-turnover cell line, and TEM revealed that the exosomes exhibited typical cup and bowl structures (Figure 2C). The exosome-specific CD63 protein and engineered GFP protein were detected on both exosomes (Figure 2D).

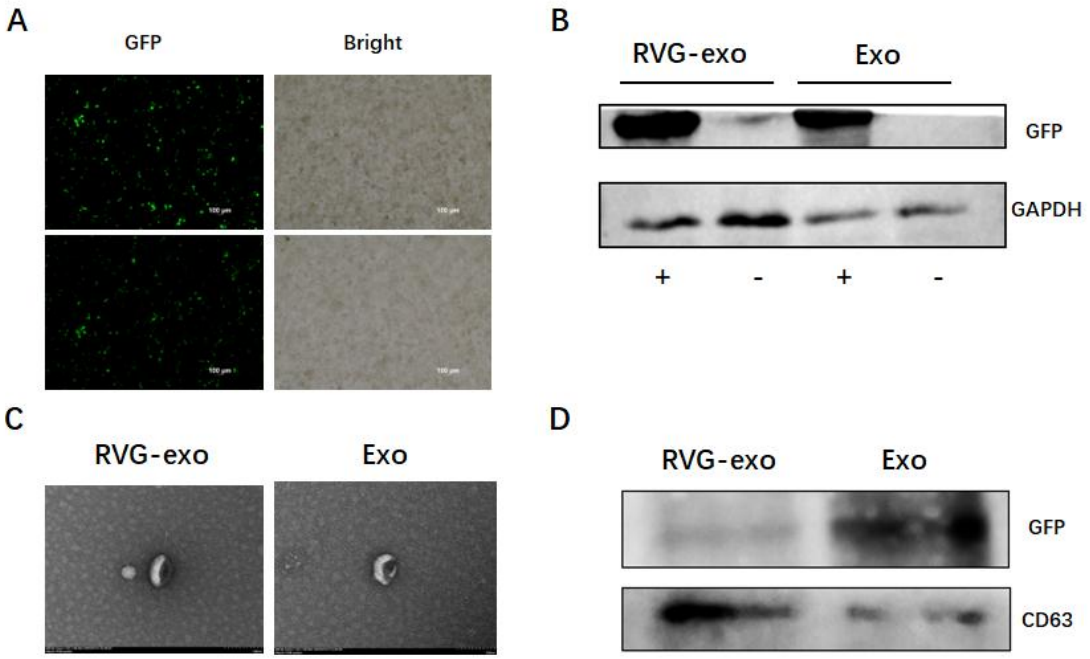

Figure 2. Identification and characterization of HEK-293 stably transduced cell lines and their exosome production. (A) Fluorescence expression of cells of two stably transfected cell lines under doxycycline induction. Scale bar: 100 μm. (B) Western blotting of the proteins of two stably transfected cell lines under doxycycline induction. (C) TEM observation of the morphology of engineered exosomes produced by two stably transduced cell lines. Scale bar: 100 nm. (D) Western blotting of engineered exosomes.

3.3. CCK-8 assay. We used a CCK-8 assay to evaluate the cytotoxicity of exosomes. Exosome complexes (phosphate-buffered saline, exosomes loaded with GAPDH siRNA [Exo/siRNA], exosomes modified with RVG and loaded with GAPDH siRNA [RVG-exo/siRNA]) at different concentrations (0, 12.5, 25, 50, and 100 μg/ml) were co-cultivated with bEnd.3 cells for 24 h. The results showed that the viability of bEnd.3 cells was not significantly affected by any exosome group, and cell viability was not significantly different from that of the control group (Figure 3).

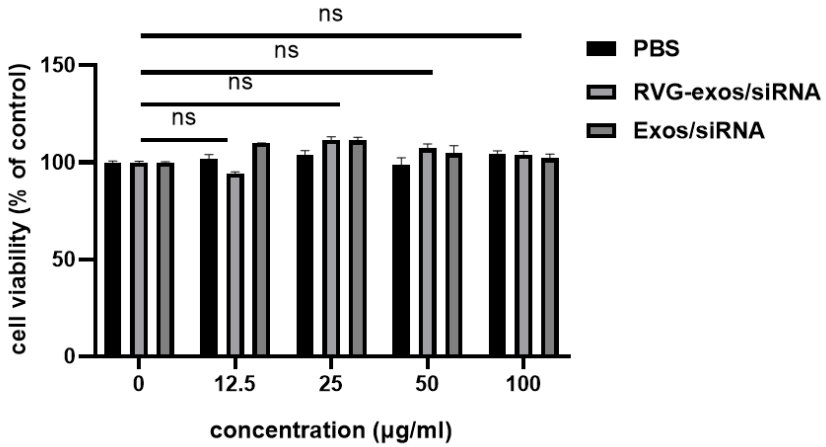

Figure 3. Cytotoxicity of engineered exosomes on bEnd.3 cells. The results of the CCK-8 assay were obtained after incubation of different concentrations of exosomes with bEnd.3 cells for 24 hours. The group with a concentration of 0 was the control group. Data are presented as the mean ± standard deviation (SD) of at least three independent experiments. Ns, $p > 0.05$.

3.4. In vitro uptake efficiency of RVG-exo. To assess the uptake efficiency of RVG-exo and Exo by bEnd.3 cells, we first assessed the difference in exosome uptake by bEnd.3 cells using a dual-fluorescent labeling strategy. After 24 h of incubation, as shown in Figure 4A, RVG-exo carrying GFP and HA tags labeled with anti-HA-Alexa Fluor 647 exhibited typical macular co-localization signals under confocal microscopy, confirming the reliability of the dual-labeling system on the surface of the exosome (Figure 4A). Partially co-localized maculae were significantly

co-localized with cells (blue). The GFP signals (green) showed higher signal intensity in the RVG-exo group, suggesting that RVG-exo was most efficiently taken up by the cells (Figure 4B). This phenomenon may be closely related to the CD46 receptor-mediated endocytosis pathway of the lattice proteins. The Alexa Fluor 647 signals (red) showed a similar trend, with the highest signals observed in RVG-exo-treated cells (Figure 4C). The difference in green and red signal intensities between the RVG-exo and exosome groups were statistically significant.

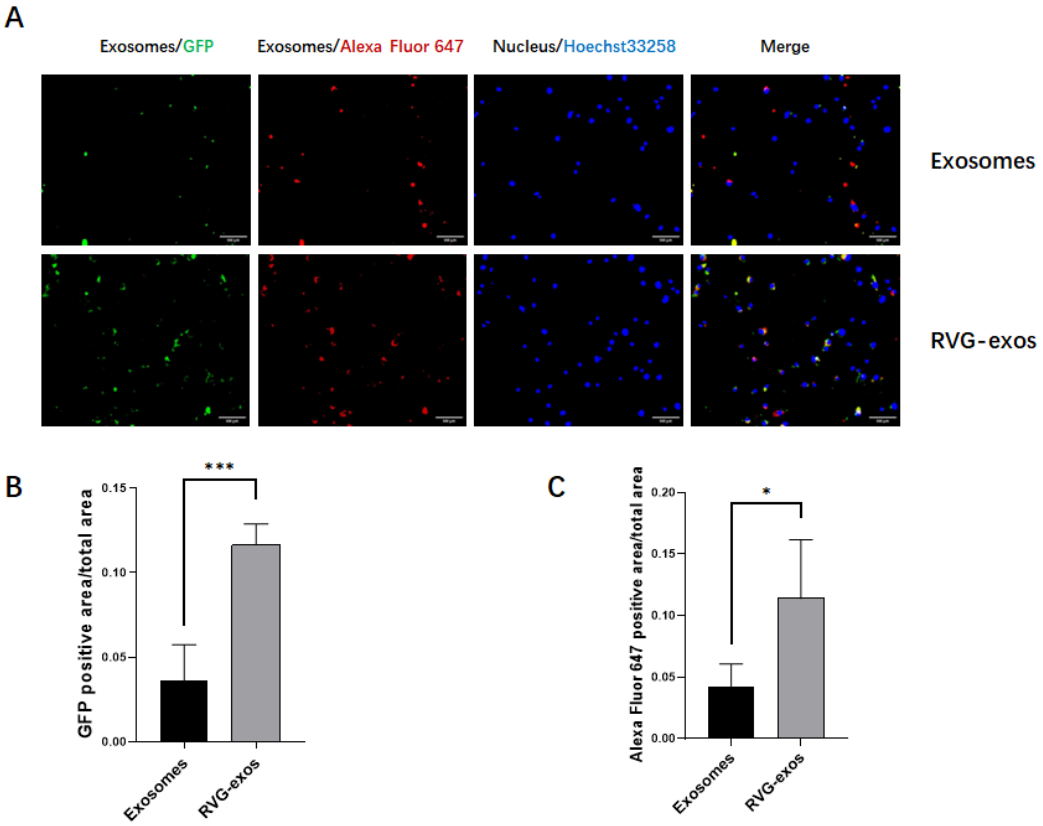

Figure 4. In vitro uptake of different exosomes. (A) GFP- and HA-labeled exosomes were co-cultured with bEnd.3 cells for 24 h. Alexa Fluor 647 was used to label HA protein on the exosomes. Cellular uptake of exosomes was observed using fluorescence microscopy. Scale bar: 100 μm. (B) Quantitative analysis of GFP-positive regions. (C) Quantitative analysis of Alexa Fluor 647-positive regions. Data are expressed as the mean ± standard deviation of three experiments. ***$p < 0.001$, *$p < 0.05$.

3.5. In vitro GAPDH siRNA delivery efficiency of RVG-exo. To assess whether exosomes loaded with siRNA can deliver their cargo precisely in vitro, we used bEnd.3 cells loaded with GAPDH siRNA into exosomes using electrotransformation. Briefly, free siRNA, liposome-complexed siRNA (Lipofectamine 6000), RVG-exos/siRNA, Exos/siRNA, and a physical mixture of RVG-exo and siRNA were incubated with bEnd.3 cells for 48 h before observing the expression of GAPDH in the cells. The results of the qPCR assay showed that the RVG-exos/siRNA group reduced the GAPDH mRNA level of bEnd.3 cells to 53%, which was significantly different from that of the control group ($p < 0.01$), not statistically different from 49% of the liposomal group ($p > 0.05$), and better than 83% of the physical mixture group, the knockdown levels of GAPDH mRNA in the Exos/siRNA group showed no statistically significant difference compared to those observed in the control group ($p > 0.05$) (Figure 5A), suggesting that exosome-mediated siRNA delivery is as effective as state-of-the-art transfection reagents. We then performed Western blotting, the results of which were consistent with the aforementioned findings (Figure 5B).

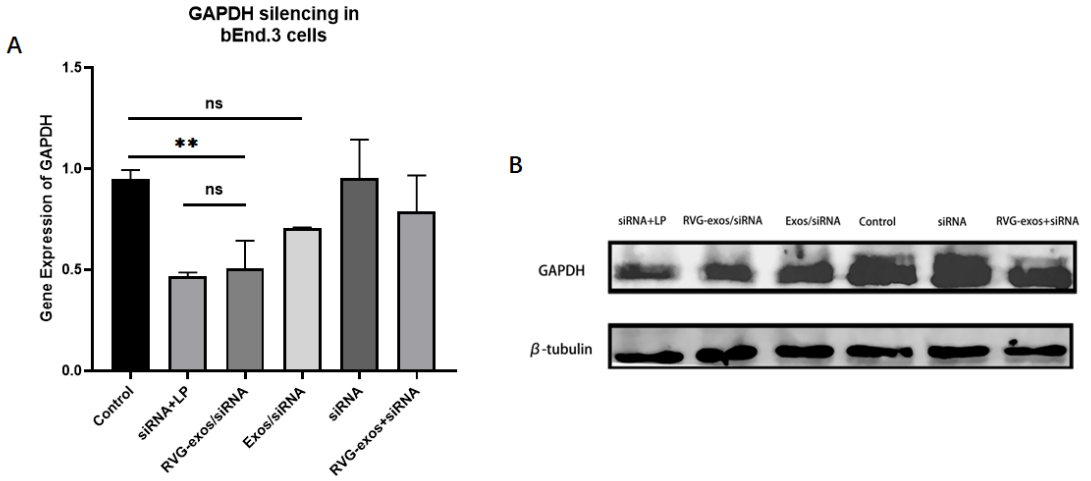

Figure 5. In vitro GAPDH siRNA delivery by different exosomes. Different exosome groups loaded with GAPDH siRNA were co-cultured with bEnd.3 cells for 48 h. (A) qPCR results of GAPDH knockdown by GAPDH siRNA. (B) Western blotting results of GAPDH siRNA against GAPDH knockdown. Data are expressed as the mean ± standard deviation of three experiments. Ns, $p > 0.05$, **$p < 0.01$.

3.6. Ability of RVG-exo to cross the BBB in vitro. We next constructed a Transwell in vitro BBB model (0.4 μm pore size) based on bEnd.3 cells to verify the trans-barrier transport properties of exo in this study system. To verify the effectiveness of the BBB model, we conducted the following experiments: a liquid level stability test and a permeability test. The liquid level stability test showed that after standing for 12 h, the initial 0.5 cm height difference between the upper chamber and the lower chamber of the BBB model remained stable (Figure 6B); The permeability test results of FITC-labelled Dextran (MW40,000) were in accordance with the in vitro permeability specification of the BBB model, and the standard curve of the FITC-dextran concentration is shown in the graph in Figure 6C. Doxorubicin (DOX) was successfully loaded into RVG-modified exosomes (RVG-exos/DOX) and unmodified exosomes (Exos/DOX) via electroporation (Figure 6A). Transmembrane transport experiments showed that the DOX fluorescence signal intensity in the lower chamber of the RVG-exos/DOX group increased with time (0–24 h) and was significantly higher than that of the Exos/DOX group at 24 h ($p < 0.001$). In the free DOX group, no apparent DOX fluorescence signal was detected in the lower chamber within 6 h, but progressive accumulation occurred thereafter. At 24 h, the signal intensity of the RVG-exos + DOX physical mixture group was comparable to that of the Exos/DOX group, but was significantly lower than that of the RVG-exos/DOX group ($p < 0.01$).

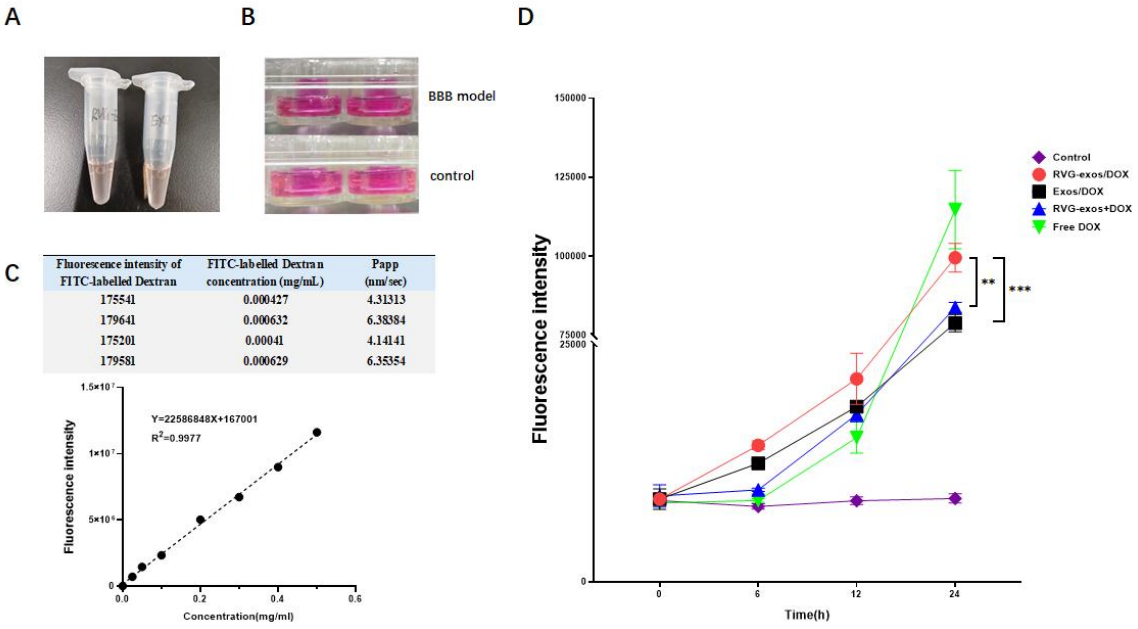

Figure 6. Different groups of exosomes loaded with Adriamycin can cross the BBB in vitro. (A) Exosomes were loaded with Adriamycin via electroporation. (B) Liquid level stability test of the BBB model. We added liquid

media to the upper and lower chambers of the constructed BBB model, maintaining a 0.5 cm height difference, and observed whether the difference in liquid level changed after 12 hours. A Transwell chamber without inoculated cells served as the control group. (C) Validation of the BBB permeability in an in vitro model. Standard curve of the FITC-labeled Dextran (MW: 40,000) concentration. (D) Intensity of Adriamycin fluorescence across the BBB at 24 h for different exosome groups loaded with Adriamycin. Data are expressed as the mean ± standard deviation of three experiments. $^{**}p < 0.01$, $^{***}p < 0.001$.

IV. DISCUSSION

Diseases of the CNS, such as AD, PD, and brain tumors, have a high prevalence worldwide, especially in older age groups. Among the neurodegenerative diseases, AD is the most common, accounting for almost 70% of all neurodegenerative diseases, and its prevalence increases with age; people over 65 years of age account for 10% of AD patients, and those over 85 years of age account for 50% [18]. Currently, there are no effective drugs for treating AD, leading it to become a hotspot for multidisciplinary research, mainly in neurology. Most patients with AD do not have a clear etiology or causative factors, and the pathogenesis has not been fully elucidated. The lesions of AD are mainly found in the medial temporal lobe, followed by the hippocampus, parahippocampal gyrus, amygdala, thalamus, posterior cingulate gyrus, and fusiform gyrus [19].

Delivering small-molecule drugs to the brain or specific neurons is the greatest challenge in AD treatment, largely due to the presence of the BBB. Although exosomes can cross the BBB to reach the substantia nigra, natural exosomes do not exhibit brain-specific targeting and do not penetrate the BBB efficiently enough to achieve therapeutic effects. Targeting peptide modification on the surface of exosomes is an effective approach to improve the targeting specificity of exosomes to the brain and the accuracy of lesion areas [20]. RVG peptide, a highly neurophilic glycoprotein with high rates of transcytosis, binds specifically to the Nicotinic acetylcholine receptor (nAChR) in the inner layer of neurons and BBB endothelial cells and crosses the BBB to increase the exosome abundance in the brain [21]. Yang Han et al. [22] developed macrophage membrane-encapsulated solid lipid nanoparticles by attaching RVG29 and triphenylphosphine cation molecules to the surface of macrophage membranes to deliver functional antioxidants to neuronal mitochondria with positive therapeutic effects on AD. Alvarez-Erviti et al. [23] reduced β-amyloid peptide aggregation by delivering BACE1 siRNA via RVG-modified exosomes to mouse brain neuroma cells. In conclusion, peptide modification can optimize the targeting of exosomes and their drug delivery capacity, reducing nonspecific drug uptake and toxicity.

In the current study, we used mouse microcerebral vascular endothelial cells and an in vitro BBB model to assess the safety, targeting efficacy, and trans-BBB ability of RVG peptide-modified exosomes. Cellular uptake assays showed that both RVG-modified exosomes (RVG-exo) and exo were taken up by cells. RVG-exo exhibited higher targeting efficacy compared with the exo, probably due to its ability to selectively bind to neurons and brain endothelial cells; this phenomenon may be closely related to CD46 receptor-mediated endocytosis of the lattice proteins pathway [24]. However, the exact mechanisms require further investigation. Compared with the in vitro cellular uptake of exosomes, their uptake in vivo is more complex. For instance, whether degradation occurs during in vivo translocation and whether RVG modification can enhance the exosome enrichment efficiency in the brain needs to be further verified.

RVG is also an effective brain-targeting agent for PD [25]. Zhang et al. [26] used RVG29 nanoparticles containing 4,4′-dimethoxy chalcone coupled with RVG29 to obtain an effective therapeutic effect against PD by crossing the BBB. Alvarez-Erviti et al. [23] demonstrated that RVG peptides were displayed on the exosome membrane protein Lamp2b after binding to the amino terminus of the exosome surface and thus have target properties. Using fusion expression of RVG, GFP, and HA to the amino terminus of the exosome membrane protein Lamp2b, we attached targeting peptides and fluorescently labeled proteins to the exosome surface before validating the reliability of this approach using TEM, western blotting, and nanoparticle size analysis. To further illustrate the effect of RVG modification on exosome targeting and drug delivery, we loaded GAPDH siRNA into exosomes via electrotransformation. We illustrated the delivery efficiency of the conjugate using fluorescence quantitative PCR and protein immunoblotting. The results showed that the GAPDH knockdown was comparable between RVG-modified exosomes and transfection reagents. By contrast, RVG-unmodified exosomes, siRNA alone, and mixtures of RVG-modified exosomes and siRNA were not significantly knocked down, suggesting that RVG modification significantly improves the efficiency of exosome delivery. Huang et al. [27] loaded siRNA into MSC-derived exosomes via electroporation to silence the *CTGF* and promote motor recovery in spinal cord-injured rats. Among the siRNA loading methods, electrotransformation has a very high loading efficiency. However, we also need to further study the loading efficiency of siRNA, study whether the morphology and size of exosomes change after electroporation, and assess the stability of siRNA after loading. We compared the ability of RVG-modified and unmodified exosomes to traverse the BBB by constructing a simple BBB model using mouse microcerebral vascular endothelial cells (bEnd.3) on Transwell membranes. We evaluated the model, and the difference in liquid level between the upper and the lower chambers did not change. We evaluated the permeability of BBB model using FITC-Glucan (MW 40,000), and the results also met the in vitro model

conditions of BBB (P_{app} between 1 and 7 nm/s) [17]. We loaded Adriamycin into exosomes to compare the fluorescence intensity across the BBB model. The results showed that both the RVG-modified and unmodified exosomes loaded with Adriamycin could cross the BBB, with fluorescence from exosome-coated doxorubicin in the lower chamber, and the signal intensity increasing over time. The RVG-exo group exhibited a higher Adriamycin signal than the Exo group, suggesting that it most effectively crossed the BBB. The free Adriamycin group and the mixture of RVG-modified exo with Adriamycin group showed no significant changes at 6 h, similar to the blank control group. In addition, the intensity of Adriamycin signals increased with time after 6 h, which could be attributed to the cellular damage induced by free Adriamycin leading to structural disruption of the BBB. The signal intensity of the physical mixture of RVG-modified exosomes with Adriamycin was slightly stronger than that of the free Adriamycin group at 6–12 h. This may be due to the partial binding of Adriamycin to the exosomes during the mixing process, but the efficiency of this binding is limited. The BBB is a highly specialized brain endothelial structure of the fully differentiated neurovascular system that separates blood from neurons in concert with pericytes, astrocytes, and microglia [28]. The BBB is not a monolithic component but a tightly connected structure of cells, including brain endothelial cells; thus, a single layer of bEnd.3 cells is insufficient to model the complex BBB structure. Furthermore, we did not evaluate the transmembrane electrical resistance value of the BBB model; thus, this component needs to be further optimized.

Although our study has some limitations, it is different from previous studies in several ways. First, we developed the RVG-GFP-Lamp2b-HA tetrameric fusion system to achieve the simultaneous optimization of exosome targeting and tracer function. Second, we established stable-translational cell lines to enable the large-scale production of engineered exosomes (with yields of up to 1–4 μg per ml of culture medium). Finally, we systematically clarified the functional relationship between exosome modification, exosome drug delivery, and multimodal exosome delivery (siRNA/small molecule drug delivery) through validation tests of exosomes. This study provides a methodological complement to existing exosome delivery strategies, as well as novel ideas for combination therapy for neurodegenerative diseases.

V. CONCLUSIONS

In this study, we developed a stable exosome-based drug delivery system. We developed two RVG-modified and unmodified exosomes, RVG-exo and exo, with GFP and constructed two stably transduced cell lines expressing RVG-exo and exo by lentiviral transduction. The two types of exosomes, RVG-exo and exo, were loaded with GAPDH siRNA and Adriamycin hydrochloride, and both RVG-modified and unmodified exosomes were well-tolerated, safe, and efficiently assimilated in vitro, with RVG-modified exosomes showing superior targeting and cross-BBB ability. The present study demonstrated that RVG-modified exosomes can significantly enhance drug efficiency across the BBB in an in vitro model, which provides data support and preclinical rationale for a novel delivery system for AD therapy. Further validation of the efficacy and long-term safety of RVG-modified exosomes in animal models is needed in the future. However, this novel delivery system for AD therapy provides a preclinical foundation for applying exosomes in the diagnosis and treatment of neurodegenerative diseases.

Acknowledgments

This work was supported by the Sichuan Science and Technology Program （2023NSFSC1149）, Science Foundation of Sichuan University of Science & Engineering (2021RC04) and Foundation of Zigong Academy of Big Data and Artificial Intelligence in Medical Science (2024-YGY-01-01). We thank LetPub (www.letpub.com.cn) for its linguistic assistance during the preparation of this manuscript.

Compliance with ethical standards

Conflict of interest

Authors declare that they have no potential conflicts of interests.

Ethical approval

This article does not contain any experiments with human participants or animals (except invertebrate's cell lines, which are exempt from ethical concerns) performed by any of the authors.

REFERENCES

[1]. Sperlágh B, Illes P. P2X7 receptor: an emerging target in central nervous system diseases[J]. Trends in Pharmacological Sciences,2014,35(10):537-547.
[2]. Zlokovic B V. The blood-brain barrier in health and chronic neurodegenerative disorders.[J]. Neuron, 2008, 57(2):178-201.
[3]. Pardridge WM. Drug transport across the blood-brain barrier[J]. J Cereb Blood Flow Metab, 2012, 32: 1959-1972.
[4]. Mathilde M ,Lorena M ,Grégory L , et al. Specificities of secretion and uptake of exosomes and other extracellular vesicles for cell-to-cell communication.[J]. Nature cell biology,2019,21(1):9-17.
[5]. Wang H, Sui HJ, Zheng Y, et al. Curcumin-primed exosomes potently ameliorate cognitive function in AD mice by inhibiting hyperphosphorylation of the Tau protein through the AKT/GSK-3beta pathway[J]. Nanoscale, 2019, 11: 7481-7496.
[6]. Rupert DLM, Claudio V, Lässer C, et al. Methods for the physical characterization and quantification of extracellular vesicles in

biological samples[J]. Biochim Biophys Acta Gen Subj, 2017, 1861: 3164-3179.
[7]. Song YY, Li ZW, He TT, Qu MJ, Jiang L, Li WL, et al. M2 microglia-derived exosomes protect the mouse brain from ischemia-reperfusion injury via exosomal miR-124[J]. Theranostics, 2019, 9(10):2910-23.
[8]. Alvarez-Erviti L, Seow Y, Yin H, Betts C, Lakhal S, Wood MJA. Delivery of siRNA to the mouse brain by systemic injection of targeted exosomes[J]. Nature Biotechnology, 2011, 29(4):341-5.
[9]. Gotti C, Clementi F. Neuronal nicotinic receptors: from structure to pathology[J]. Progress in Neurobiology, 2004, 74(6):363-96.
[10]. Osakada F, Callaway EM. Design and generation of recombinant rabies virus vectors[J]. Nature Protocols, 2013, 8(8):1583-601.
[11]. Fu C, Xiang Y, Li X, Fu A. Targeted transport of nanocarriers into brain for theranosis with rabies virus glycoprotein-derived peptide[J]. Materials Science and Engineering: C, 2018, 87:155-66.
[12]. Mizrahy S, Gutkin A, Decuzzi P, Peer D. Targeting central nervous system pathologies with nanomedicines[J]. Journal of Drug Targeting, 2018, 27(5-6):542-54.
[13]. Kumar P, Wu H, McBride JL, Jung K-E, Hee Kim M, Davidson BL, et al. Transvascular delivery of small interfering RNA to the central nervous system[J]. Nature, 2007, 448(7149):39-43.
[14]. Xiang L, Zhou R, Fu A, Xu X, Huang Y, Hu C. Targeted delivery of large fusion protein into hippocampal neurons by systemic administration[J]. Journal of Drug Targeting, 2010, 19(8):632-6.
[15]. Hwang DW, Son S, Jang J, Youn H, Lee S, Lee D, et al. A brain-targeted rabies virus glycoprotein-disulfide linked PEI nanocarrier for delivery of neurogenic microRNA[J]. Biomaterials, 2011, 32(21):4968-75.
[16]. Hong W, Zhang Z, Liu L, Zhao Y, Zhang D, Liu M. Brain-targeted delivery of PEGylated nano-bacitracin A against Penicillin-sensitive and -resistant Pneumococcal meningitis: formulated with RVG29 and Pluronic® P85 unimers[J]. Drug Delivery, 2018, 25(1):1886-97.
[17]. Irvine JD, Takahashi L, Lockhart K, Cheong J, Tolan JW, Selick HE, Grove JR. MDCK (Madin–Darby canine kidney) cells: a tool for membrane permeability screening. Journal of pharmaceutical sciences. 1999 Jan;88(1):28-33.
[18]. Zvěřová, M. (2019) Clinical Aspects of Alzheimer's Disease. Clinical Biochemistry, 72, 3-6.
[19]. Butcher, H.K., Holkup, P.A. and Buckwalter, K.C. (2001) The Experience of Caring for a Family Member with Alzheimer's Disease. Western Journal of Nursing Research, 23, 33-55.
[20]. Kim, G.; Kim, M.; Lee, Y.; Byun, J. W.; Hwang, D. W.; Lee, M. Systemic delivery of microRNA-21 antisense oligonucleotides to the brain using T7-peptide decorated exosomes. J. Controlled Release 2020, 317, 273−281.
[21]. You, L.; Wang, J.; Liu, T.; Zhang, Y.; Han, X.; Wang, T.; Guo,S.; Dong, T.; Xu, J.; Anderson, G. J.; Liu, Q.; Chang, Y. Z.; Lou, X.;Nie, G. Targeted Brain Delivery of Rabies Virus Glycoprotein 29 Modified Deferoxamine-Loaded Nanoparticles Reverses Functional Deficits in Parkinsonian Mice. ACS Nano 2018, 12 (5), 4123−4139.
[22]. Yang H, Chunhong G ,Hao W , et al. Corrigendum to "Macrophage membrane-coated nanocarriers Co-Modified by RVG29 and TPP improve brain neuronal mitochondria-targeting and therapeutic efficacy in Alzheimer's disease mice" [Bioactive materials 6 (2021) 529-542].[J].Bioactive materials,2022,773-73.
[23]. Lydia A, Yiqi S, Haifang Y, et al. Delivery of siRNA to the mouse brain by systemic injection of targeted exosomes.[J].Nature biotechnology,2011,29(4):341-5.
[24]. Kuroda H, Tachikawa M, Yagi Y, et al. Cluster of differentiation 46 is the major receptor in human blood-brain barrier endothelial cells for uptake of exosomes derived from brain-metastatic melanoma cells (SK-Mel-28)[J]. Mol Pharm, 2019, 16: 292-304.
[25]. Han, Y.; Gao, C.; Wang, H.; Sun, J.; Liang, M.; Feng, Y.; Liu,Q.; Fu, S.; Cui, L.; Gao, C.; Li, Y.; Yang, Y.; Sun, B. Macrophage membrane-coated nanocarriers Co-Modified by RVG29 and TPP improve brain neuronal mitochondria-targeting and therapeutic efficacy in Alzheimer's disease mice. Bioact. Mater. 2021, 6 (2),529−542.
[26]. Wenlong Z, Huaqing C, Liuyan D, et al.Trojan Horse Delivery of 4,4′-Dimethoxychalcone for Parkinsonian Neuroprotection[J].Advanced Science,2021,8(9):2004555-2004555.
[27]. Wei H ,Mingjia Q ,Lu L , et al.SiRNA in MSC-derived exosomes silences CTGF gene for locomotor recovery in spinal cord injury rats[J].Stem Cell Research & Therapy,2021,12(1):334-334.
[28]. Zlokovic V B .The Blood-Brain Barrier in Health and Chronic Neurodegenerative Disorders[J].Neuron,2008,57(2):178-201.